Sono-synthesized sword-like zinc oxide and its use as a filler in polyurethane composites

C. PHOLNAK, C. SIRISATHITKUL[*], S. DANWORAPHONG, D. J. HARDING
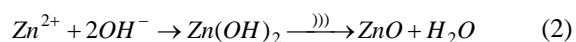*Molecular Technology Research Unit, School of Science, Walailak University, Nakhon Si Thammarat, 80161 Thailand*

Zinc oxide (ZnO) particles with sword-like morphology were sonochemically synthesized from $Zn(NO_3)_2$–$C_6H_{12}N_4$ aqueous solutions at 90°C. After the crystal growth, the ultrasonic irradiation facilitates the erosion process at the ends of hexagonal ZnO rods resulting in a sword-like morphology and reduces the overall crystal size. Increasing the ratio of $C_6H_{12}N_4$ to $Zn(NO_3)_2$ from 1:2 to 5:1 increases the density of sword-like ZnO clusters. An extra absorption peak in the ultraviolet (UV) regime is observed in commercial polyurethane loaded with the surface modified ZnO. The dispersion of 15 wt% ZnO gives rise to a stronger UV absorption than that by 5 wt% ZnO.

1. Introduction

Recent years have seen extensive research into ZnO micro- and nanostructures because of the potential applications in catalysis, electronics, photonics and medicine [1-3]. Potential devices include light emitting diodes, lasers, dye sensitized solar cells, piezoelectric generators, gas sensors and microwave absorbers [4-6]. The morphology and size of the ZnO particles is found to greatly influence their suitability for a particular application and controllable synthesis is thus essential. ZnO can now be synthesized in different morphologies by a variety of techniques including chemical solution route, thermal evaporation, vapor phase transport, hydrothermal, sol-gel, microwave-assisted and sonochemical synthesis [7,8]. In the sonochemical method, ultrasound waves supply the high energy needed for chemical reactions via the process of acoustic cavitations involving the formation, growth and implosive collapse of bubbles in the liquid. During the cavitational collapse of the bubbles, intense local heating occurs for a few microseconds resulting in high-velocity interparticle collisions whose impact can be used in the following reactions [9].

$$Zn^{2+} + 4OH^- \rightarrow Zn(OH)_4^{2-} \xrightarrow{\;)))\;} ZnO + H_2O + 2OH^- \quad (1)$$

$$Zn^{2+} + 2OH^- \rightarrow Zn(OH)_2 \xrightarrow{\;)))\;} ZnO + H_2O \quad (2)$$

Like other methods, ZnO of different shapes have been obtained from sonochemical synthesis such as spheres [10], flower-like [10], cauliflower-like [11], octahedron [12], nanosheets [13], and nanorods [10,14]. Jung *et al.* summarized the evolution of the sonosynthesized ZnO nuclei into spheres (isotropic growth), disks (suppression of 1-D growth), rods (1-D growth) and flower-like ZnO (multiple nanorods growth)

[10]. Furthermore, it has been found that ultrasonic facilitates the erosion at the end of ZnO rods resulting in hexagonal tubes or cups [10,15]. Interestingly, the erosion of the end of ZnO rods can result in a sword-like morphology when microwave-assisted synthesis is used [16].

Nanocomposites involve the incorporation of inorganic fillers typically, into a polymer. The nanocompsites often have novel properties not present in either of the pure materials. Polyurethane (PU) has been used in the preparation of nanocomposites and is extremely versatile due to the wide variety of raw materials that may be used [17]. In the case of ZnO filled PU composite materials, different morphology ZnO results in modification of the physical and mechanical properties of this material as well as an effective improvement for a range of attractive applications. For instance, the anti-oxidation properties of PU are enhanced by 1% ZnO nanoparticles and the corrosion resistance when applied to the surface of an aluminum alloy is attributed to the "labyrinth" effect of the nano-network [18]. Tetrapod-shape ZnO whiskers act as effective conducting additives in the antistatic mechanism of ZnO coated PU because of the charge concentrating effect at the tips of the whisker and the possible existence of a tunneling effect resulting in lowering of the electrical resistivity in the composites [19]. In the same morphology, PU coated films containing 20-40 wt% of tetrapod ZnO exhibit microwave absorption and microwave-heat transformation in the frequency of 14-18 GHz (Ku-band) associated with the tetra-needle shape, diffuse reflections result from quasi-antenna, multipoles due to the charge concentration and the multi-interfaces in the composites [20]. Flower-like ZnO nanowhiskers (f-ZnO) showed an intense effect on the mechanical properties of PU composite films increasing the tensile strength significantly up to an optimal value of 1.0 wt% due to the reinforcing effect of the f-ZnO network

structure. More importantly, the composite films with 4.0 wt% of f-ZnO exhibited strong antibacterial activities against *E. coli* and *S. aureus* [21]. It is clear from these results, that PU/ZnO composites are potentially useful in a variety of coating applications.

In this paper we report the effect of the concentration of the starting materials and the temperature on the morphology of the sonochemically prepared ZnO. Moreover, we also examine how the amount of sword-like ZnO powder in the PU affects the optical properties of the nanocomposites.

2. Experimental

The sonicator used in this work is an 800 ml metallic cube with parallel, dual stack PZT transducers attached on two faces as shown in Fig. 1. These transducers were sinusoidally driven by a function generator at 35 kHz with a 100 W power amplifier. The cube was placed on a hot plate with a magnetic stirrer. In the synthesis of ZnO, aqueous solutions of zinc nitrate and hexamethylenetetramine were prepared separately by adding $Zn(NO_3)_2 \cdot 6H_2O$ (0.05 M, 11.90 g) and $C_6H_{12}N_4$

(0.05 M, 5.61 g) into 400 ml deionized water in glass beakers under stirring for 10 min at room temperature. Both solutions were then mixed in the sonicator under vigorous stirring (1000 rpm) and heated to 50°C. Once the solution turned to a stable viscous white colloid, the stirring was continued for another 10 min. Three samples were initially prepared according to this procedure and then each sample was heated to its final temperature, 70, 80 and 90°C before being sonicated for 60 min. The samples were then compared with those synthesized at the same temperatures without sonication to justify the effect of ultrasonic irradiation at varying temperatures. To investigate the effect of reagent concentration, three more samples were prepared by varying the concentration of the $C_6H_{12}N_4$ solution (0.025, 0.1 and 0.25 M) and keeping the $Zn(NO_3)_2 \cdot 6H_2O$ concentration at 0.05 M with 60 min irradiation at 90°C. After each reaction was complete, the white precipitate was collected by filtration and thoroughly rinsed with distilled water and ethanol. Finally, the precipitate was dried in an oven at 100 °C in an air atmosphere for 2 h. The size and morphology of the ZnO powders were inspected by scanning electron microscopy (SEM, FEI Quanta 400) operating at 25 kV.
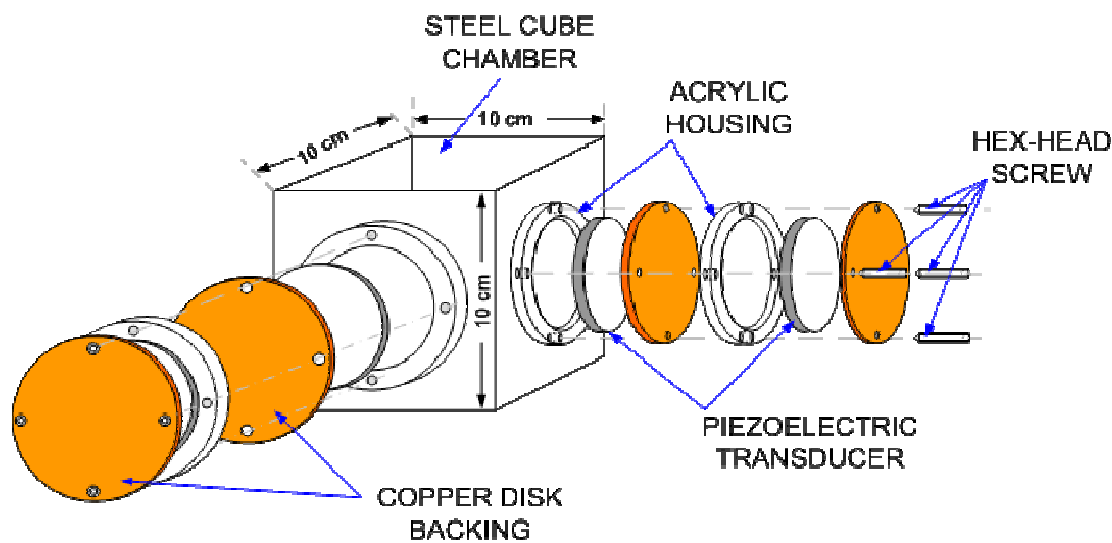

Fig. 1. Schematic diagram of the sonicator.

In order to enhance the dispersion of ZnO powder into the PU matrix, its surface was modified with γ-aminopropyltriethoxysilane as a coupling agent prior to the incorporation. The ZnO powder was dried in an oven at 120 °C for 18 h and the coupling agent was dissolved in ethanol in a volume ratio of 1:50. They were mixed in a weight ratio of solution to ZnO of 6:100. The mixture was stirred (60 rpm) for 2 h at 40 °C. It was then heated up to the boiling point of ethanol, 78°C, and further stirred until the ethanol was completely evaporated (~6 h). Finally, the surface modified ZnO was dried in an oven at 120°C for 18 h. The commercial grade PU clear coat (S-3000, TOA, Thailand) was used by diluting with 30% (v/v) PU thinner

(TOA, Thailand) to reduce the viscosity and amount of bubbles of the coating solution. The solution was stirred at room temperature for 5 min. Then, 1 and 3 g of the surface modified ZnO filler were dispersed into 20 ml (20.69 g) diluted PU solutions corresponding to 5 and 15% (w/v). The colloids were stirred (80 rpm) for 6 h under ambient conditions.

Before using as a substrate, a thick polypropylene (PP) sheet (75 mm × 25 mm × 1 mm) was gently cleaned with ethanol. The film deposition was carried out in an air atmosphere at room temperature by dip coating. The PP substrate was dipped in the ZnO colloid and then pulled up at a speed of 1 cm/min by using a computer-interfaced long travel stage (LTS150, Thorlabs). The dip-coated

films with 5 and 15% (w/v) ZnO were left for 24 h to dry at room temperature under an air atmosphere. X-ray diffraction (XRD, Philips X′ Pert MPD) of the films was carried out with Cu$K\alpha$ radiation (λ = 1.540 Å). Their optical absorption spectra were measured on an ultraviolet-visible (UV-Vis) spectrophotometer (Shimadzu, UV-1700) with a double beam system of halogen and deuterium light sources.

3. Results and discussion

The phase and morphology of all nine samples are summarized in Table 1. Whereas the crystallographic structure of every sample is hexagonal wurtzite ZnO, its morphology varies with the reaction temperature, reagent concentration and ultrasonic irradiation. In Fig. 2, the SEM micrographs of the three ZnO samples prepared without the use of ultrasound waves are shown. Hexagonal prisms with a length of about 360 nm and a width ranging from 120 to 240 nm were obtained in the case of 70°C in Fig. 2(a). By increasing the temperature up to 80°C, the ZnO prisms grow larger during the same 60 min period. Moreover, the majority of these hexagonal rods cross one another to form clusters. When the temperature is increased to 90°C, clusters of linked rods of about 6.8 μm in diameter are obtained as seen in Fig. 2(c). It is noted that the end of the rods start to decompose and the hexagonal cross section becomes smaller.

Table 1 *Effect of the sonication, temperatures and concentrations of the reagent on the phase and morphology of ZnO products.*

Sonication Time (min)	Reaction Time (min)	Temperature (°C)	Concentration (M)		Crystalline phase	Morphology
			$Zn(NO_3)_2 \cdot 6H_2O$	$C_6H_{12}N_4$		
0	60	70	0.05	0.05	ZnO	Hexagonal prisms
0	60	80	0.05	0.05	ZnO	Hexagonal linked rods
0	60	90	0.05	0.05	ZnO	Hexagonal linked rods
---	---	---	---	---	---	---
60	60	70	0.05	0.05	ZnO	Hexagonal prisms
60	60	80	0.05	0.05	ZnO	Hexagonal linked rods
60	60	90	0.05	0.05	ZnO	Sword-like
---	---	---	---	---	---	---
60	60	90	0.05	0.025	ZnO	Sword-like
60	60	90	0.05	0.1	ZnO	Sword-like
60	60	90	0.05	0.25	ZnO	Sword-like

The formation processes of ZnO whose morphology is shown in Fig. 2 can be explained as follows. Since the crystal formation is divided into crystal nucleation and growth stages, the obtained particle size and shape depend on the nucleation rate and crystal growth rate. A lot of ZnO nuclei form at the beginning. Zinc cations are known to readily react with hydroxide anions to form stable $Zn(OH)_4^{2-}$ complexes which act as the growth unit of ZnO nanostructures. Driven by the surface energy as well as Coulombic forces, some ZnO nuclei suddenly aggregate. Zhang *et al.* showed that the variation in temperature of chemical solutions led to either prickly spheres or rod shaped ZnO [22].

In the case of nanorods, ZnO nanocrystals grow preferentially along the c-axis. After that, each core grows anisotropic along its [0001] direction. Hence this morphology comprises several single crystals rapidly extending from the core [10,23].

The microprism and hexagonal rods have a flat hexagonal top face upon the Zn surface that are formed with the six crystallographic planes representing the typical hexagonal wurtzite type lattice. Yang *et al.* have suggested that the positive-face (0001) and negative-face (000$\bar{1}$) are metastable states and they are susceptible to erosion into hollow tubes after prolonged chemical reactions [24].
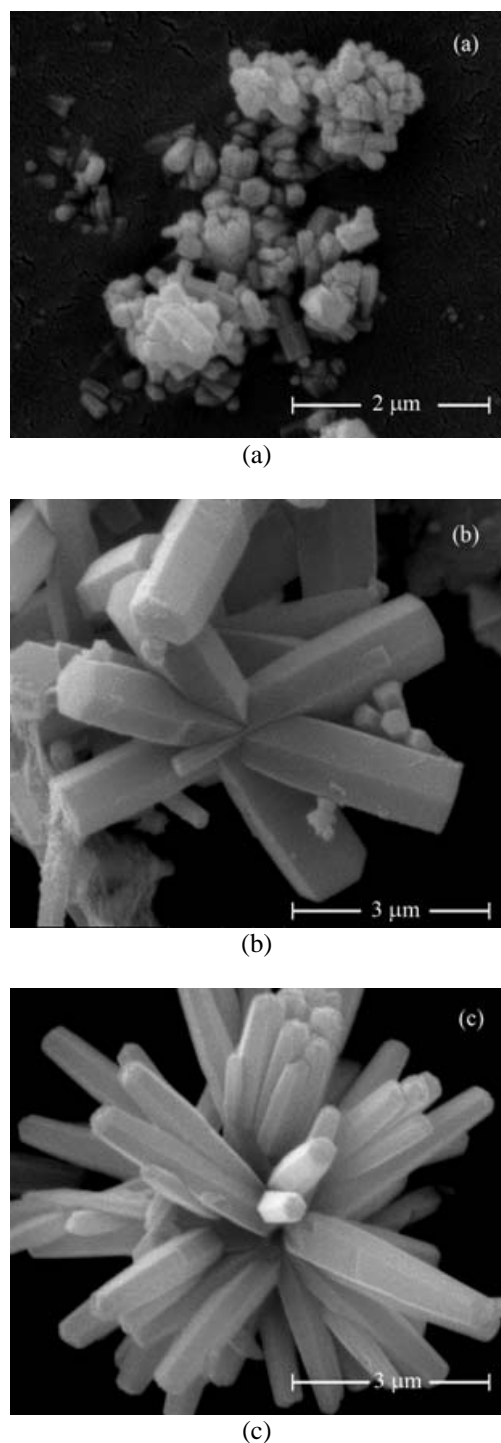
(a)

(b)

(c)

Fig. 2. SEM micrographs of ZnO products from 0.05 M Zn(NO₃)₂–C₆H₁₂N₄ aqueous solution without sonication at (a) 70 °C, (b) 80 °C and (c) 90 °C.

The morphology of sono-synthesized ZnO as shown in Fig. 3 is different from that of unsonicated ZnO at identical temperatures. It also depends on the temperature in the aqueous solution during ultrasonic irradiation. In the case of 70°C, clusters of hexagonal prisms of ZnO with a length of *ca.* 300 nm are observed. The length of the ZnO prisms is increased with an increase in the reaction temperature similar to the trend in unsonicated ZnO but there is no substantial increase in the diameter. When the temperature is increased to 80°C, ZnO becomes linked rods *ca.* 700 nm in length which are much smaller than those obtained without sonication. At 90°C, the clusters of hexagonal rods develop into aggregated sword-like ZnO with diameters around 3 μm and rounded tips indicating that the decomposition is more pronounced due to sonication. Results from the comparison emphasize the role of ultrasonic irradiation in the sword-like morphology and overall reductions in the crystal size.

Whereas heating Zn(NO₃)₂–C₆H₁₂N₄ aqueous solutions could form ZnO hexagonal rods, the sonication is vital in the preparation of linked nanorods and sword-like ZnO. The difference between SEM images in Figs. 2 and 3 emphasizes the influence of sonication on the ZnO morphology. The acoustic cavitation is based on three steps consisting of nucleation, growth and implosive collapse of bubbles. The energy in the final step and surrounding liquid molecules leads to the erosion at the end of the nanorods [16]. For the reaction with sword-like ZnO clusters, both nucleation and growth processes occur rapidly. When the growth process stops, the erosion process subsequently begins resulting in Fig. 3(c). Adapted from the formation mechanism of nanotubes [24], it can be proposed that the end of each hexagonal rod is eroded through continuous sonication at high temperature and sword-like ZnO structures are then formed. The time of sonication is likely to play a critical role in determining the morphology of ZnO. Interestingly, Wahab *et al.* obtained needle-like ZnO after the 40 kHz sonication of zinc acetate dihydrate and sodium hydroxide for 120 min [9]. With 0.005 M Zn(NO₃)₂ and 0.005 M C₆H₁₂N₄ as starting materials Hu *et al.* observed ZnO linked nanorods using a 20 kHz sonicator for 30 min [25].

The morphology of samples prepared from different concentrations of C₆H₁₂N₄ reagent (ratio of $[OH^-:Zn^{2+}]$ = 1:2, 2:1 and 5:1) sonicated at 90°C is shown in Figs. 3(d)-(f). The same sword-like morphology may be observed, but the density of ZnO clusters significantly increases by increasing the concentration of C₆H₁₂N₄. Moreover, the length of single sword-like rod is shortened from 1.2 μm in Fig. 3(d) to 650 nm in Fig. 3(f). The results agree with the trend observed by Yang *et al.* in nanorods from the same starting materials without sonication [24]. The decomposition of C₆H₁₂N₄ can be expressed in the following reactions.

$$C_6H_{12}N_4 + 6H_2O \rightarrow 4NH_3 + 6HCHO \qquad (3)$$

$$NH_3 + H_2O \rightarrow NH_4^+ + OH^- \qquad (4)$$

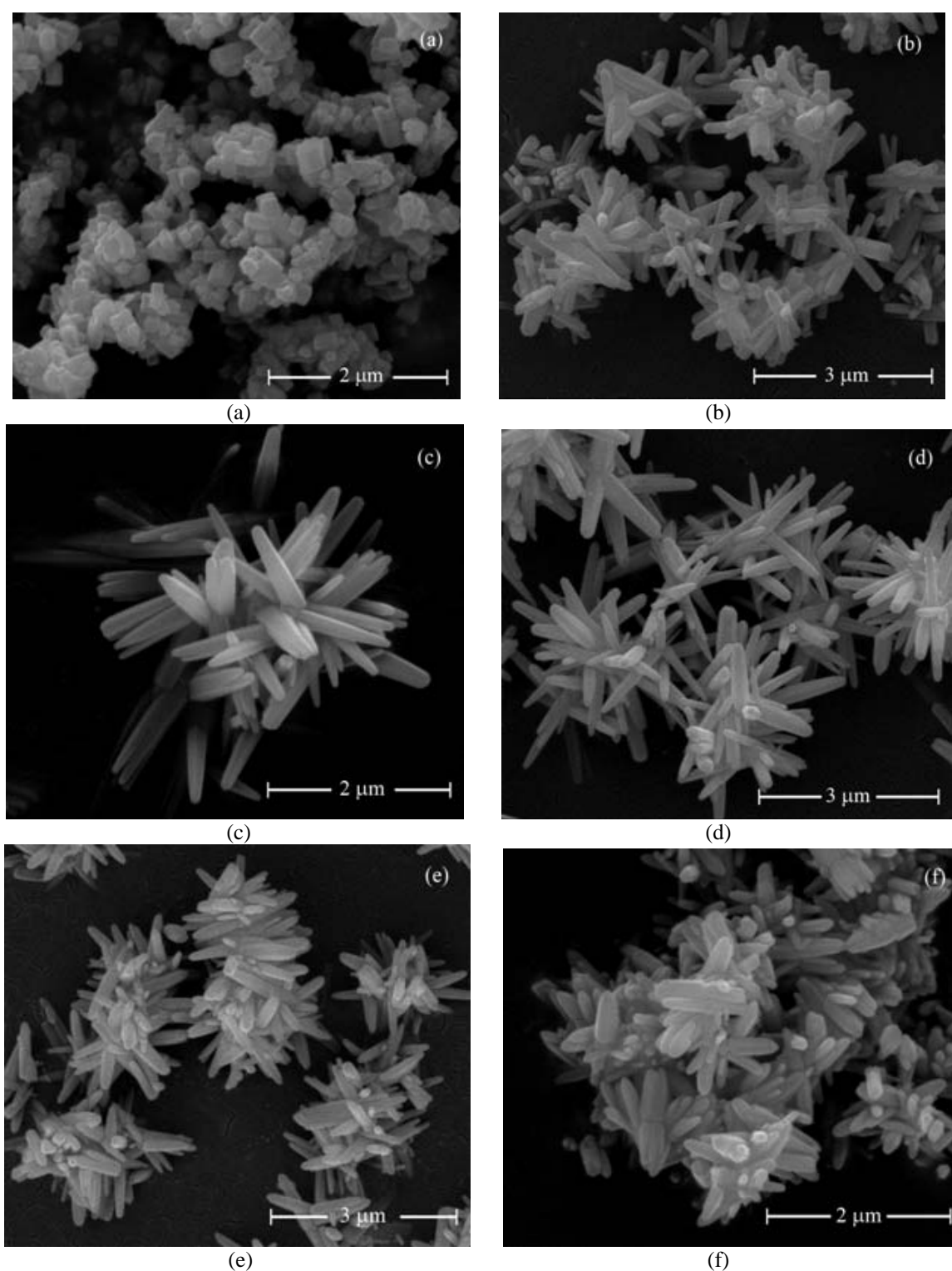*Fig. 3. SEM micrographs of ZnO products from sonicated $Zn(NO_3)_2–C_6H_{12}N_4$ aqueous solution at varying temperatures [(a) 70 ℃, (b) 80 ℃, (c) 90 ℃] with a ratio of $C_6H_{12}N_4$ to $Zn(NO_3)_2$ 1:1 and with varying ratio of $C_6H_{12}N_4$ to $Zn(NO_3)_2$ [(d) 1:2, (e) 2:1 (f) 5:1] at 90 ℃.*

The abundant NH_4^+ and OH^- ions from the hydration of $C_6H_{12}N_4$ play a key role in the formation of nano-ZnO crystals. The supersaturated OH^- ions react with Zn^{2+} following the chemical reactions in Eq. (1)-(2). The increased yield of products may be due to an increase in the probability of interaction between Zn^{2+} and OH^- ions by the sonochemical effect which is the same mechanism in the case of less concentrated reagents [24].
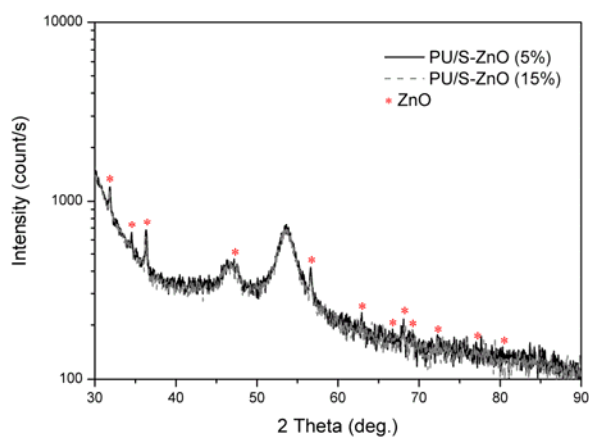

Fig. 4. XRD patterns of the PU films filled with 5 wt% (black solid line) and 15 wt% (gray dashed line) sword-like ZnO.
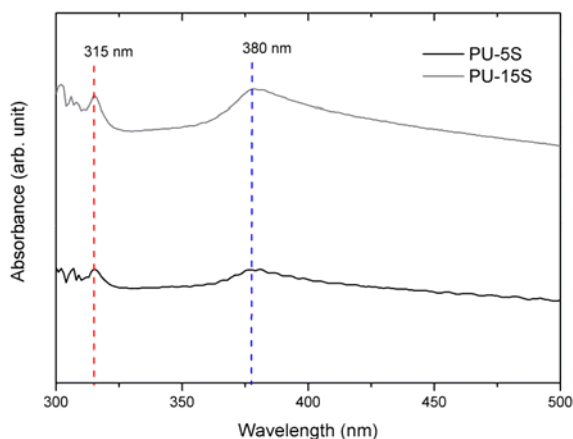

Fig. 5. UV-Vis absorption spectra of the PU films filled with 5 wt% (black line) and 15 wt% (gray line) sword-like ZnO.

The XRD patterns of the two PP sheets coated by PU/ZnO composites are shown in Fig. 4. All indexed peaks belong to the ZnO fillers with a space group of P63mc (ICPDF No. 01-089-0511) whereas other peaks originate from either the PP substrate or PU coating. XRD patterns in the case of 5% and 15% sword-like ZnO are comparable and clearly confirm the presence of ZnO in the PU films. UV-Vis absorbance spectra of the PU composite films filled with surface modified sword-like ZnO fillers are shown in Fig. 5. The absorbance spectra in the case of 5 wt% have two bands; one broad band centered at 380 nm

and the other around 315 nm. The former, also seen from ZnO in other shapes and sizes [9,12,26,27], is associated with the intrinsic band gap of ZnO. The latter, a small but sharp peak, is possibly attributed to the band edge absorption of sword-like ZnO [28]. This extra UV absorption peak is present in all samples loaded with the sword-like ZnO. In the PU films containing 15 wt% ZnO fillers, the intensity of both peaks is higher indicating increased UV absorption by ZnO.

4. Conclusions

We have shown that the application of ultrasonic waves during the synthesis of ZnO crystals causes significant changes in the crystal size and morphology. To single out the effect of the sonication, a comparison between the samples prepared by a temperature dependent method and those obtained by applying a constant ultrasound field was made. In addition, reagent concentrations were also varied under the same ultrasound irradiation conditions. The ZnO crystals prepared with the aid of ultrasound show dramatic decreases in overall size and the occurrence of the sword-like morphology can be clearly seen for crystals prepared at 90°C. Moreover, the concentration of the reagent also affects the size and the density of the crystal cluster. The higher the concentration the smaller and the denser the crystal clusters. After incorporation of these sword-like ZnO into PU, the composites exhibit an extra UV absorption peak along with that corresponding to bulk ZnO.

References

[1] Z.L. Wang, Chin. Sci. Bull. **54**, 4021 (2009).
[2] J.S. Wu, D.F. Xue, Sci. Adv. Mater. **3**, 127 (2011).
[3] P. Gowthaman, M. Saroja, M. Venkatachalam, J. Deenathayalan, T.S. Senthil, Optoelectron. Adv. Mater. Rapid Commun. **13**, 631 (2011).
[4] A.B. Djurisic, A.M.C. Ng, X.Y. Chen, Prog. Quan. Electron. **34**, 191 (2010).
[5] A. Wei, L.H. Pan, W. Huang, Mater. Sci. Eng. B **176**, 1409 (2011).
[6] X.-L. Du, Y. Sun, Q. Wang, N. Ma, Z.-H. Yuan, J. Optoelectron. Adv. Mater. **13**, 631 (2011).
[7] S.J. Pearton, D.P. Norton, K. Ip, Y.W. Heo, T. Steiner, Prog. Mater Sci. **50**, 293 (2005).
[8] X. Wang, Y. Wang, J. Jia, Y. Tian, L. Zhang, J. Optoelectron. Adv. Mater. **13**, 227 (2011).

[9] R. Wahab, S.G. Ansari, Y.-S. Kim, H.-K. Seo, H.-S. Shin, Appl. Surf. Sci. **253**, 7622 (2007).

[10] S.H. Jung, E. Oh, K.H. Lee, Y. Yang, C.G. Park, W.J. Park, S.H. Jeong, Cryst. Growth Des., **8** 265 (2008).

[11] M. Mazloumi, S. Zanganeh, A. Kajbafvala, P. Ghariniyat, S. Taghavi, A .Lak, M. Mohajerani, S.K. Sadrnezhaad, Ultrason. Sonochem. **16**, 11 (2009).

[12] C. Pholnak, C. Sirisathitkul, D.J. Harding, J. Phys. Chem. Solids **72**, 817 (2011).

[13] Q. Xiao, S. Huang, J. Zhang, C. Xiao, X. Tan, J. Alloys Compd. **459**, L18 (2008).

[14] K. Uma, S. Ananthakumar, R.V. Mangalaraja, K.P.O. Mahesh, T. Soga, T. Jimbo, J. Sol-Gel Sci. Technol. **49**, 1 (2009).

[15] C. Pholnak, C. Sirisathitkul, D.J. Harding, S. Suwanboon, J. Ceram. Soc. Jpn. **119**, 35 (2011).

[16] A. Kajbafvala, M.R. Shayegh, M. Mazloumi, S. Zanganeh, A. Lak, M.S. Mohajerani, S.K. Sadrnezhaad, J. Alloys Compd. **469**, 293 (2009).

[17] S.A. Madbouly, J.U. Otaigbe, Prog. Polym. Sci. **34**, 1283 (2009).

[18] Z. Wang, F. Liu, E. Han, W. Ke, S. Luo, Chin. Sci. Bull. **54**, 3464 (2009).

[19] Z. Zhou, L. Chu, W. Tang, L. Gu, J. Electrostat., **57**, 347 (2003).

[20] Z. Zhou, L. Chu, S. Hu, Mater. Sci. Eng. B **126**, 93 (2006).

[21] X.-Y. Ma, W.-D. Zhang, Polym. Degrad. Stabil. **94**, 1103 (2009).

[22] J. Zhang, L. Sun, J. Lin, H. Su, C. Liao, C. Yan, Chem. Mater. **14**, 4172 (2002).

[23] J. Xie, P. Li, Y. Wang, Y. Wei, J. Phys. Chem. Solids **70**,112 (2009).

[24] J. Yang, J. Lang, L. Yang, Y. Zhang, D. Wang, H. Fan, H. Liu, Y. Wang, M. Gao, J. Alloys Compd. **450**, 521 (2008).

[25] X.-L. Hu, Y.-J. Zhu, S.-W. Wang, Mater. Chem. Phys. **88**, 421 (2004).

[26] L. Wu, Y. Wu, J. Mater. Sci. **42**, 406 (2007).

[27] R.S. Yadev, P. Mishra, A.V. Pandey, Ultrason. Sonochem. **15**, 863 (2008).

[28] L. Kumari, W.Z. Li, Cryst. Res. Technol. **45**, 311 (2010).

_____

*Corresponding author: schitnar@wu.ac.th